Excited Mixed-Valence States of Symmetrical Donor−Acceptor−Donor π Systems

Stephan Amthor,[†] Christoph Lambert,*[,†] Stefan Dümmler,[‡] Ingo Fischer,*[,‡] and Jürgen Schelter[†]

Institut für Organische Chemie, and Institut für Physikalische Chemie, Bayerische Julius-Maximilans-Universität Würzburg, Am Hubland, D-97074 Würzburg

Received: November 21, 2005; In Final Form: February 10, 2006

We investigated the spectroscopic properties of a series of four bistriarylamine donor−π−bridge-donor D−π−D compounds (dimers), composed of two asymmetric triarylamine chromophores (monomers). UV/vis, fluorescence, and transient absorption spectra were recorded and compared with those of the corresponding D-π monomers. Bilinear Lippert−Mataga plots indicate a major molecular reorganization of the excited state in polar media for all compounds. The excited states of the dimers are described as mixed-valence states that show, depending on the chemical nature of the π bridge, a varying amount of interactions (couplings). We found that superradiant emission, that is, an enhancement of the fluorescence rate in the dimer, is observed only in the case of weak and medium coupling. Whether the first excited-state potential energy surface of the dimers is described by single minimum or a double minimum potential depends on the solvent polarity and the electronic coupling. In the latter case, the dimer relaxes in a symmetry broken CT state with partial positive charge at the triarylamine donor and negative charge at the π bridge. The [2.2]paracyclophane bridged dimer is an example of a weakly coupled system because the spectroscopic behavior is very similar to the corresponding *p*-xylene monomer. In contrast, anthracene as well as *p*-xylene bridges mediate a stronger coupling and reveal a significant cooperative influence on the optical properties.

Introduction

The donor−π−bridge-donor (D−π−D) motive plays an increasingly important role in conjugated π-electron systems for two-photon absorption applications.[1−10] For a rational design of optoelectronic properties, it is necessary for one to develop models that describe most if not all of the ground- and excited-state features of these D−π−D chromophores. In this paper we use spectroscopic information to develop such a model for a number of D−π−D systems in which the donors are triarylamine groups at a constant separation while the chemical nature of the π bridge varies. We construct the excited-state potential energy surfaces for these D−π−D chromophores within the framework of a three-state model and explain the photophysical behavior. Furthermore, we show that the electronic nature of the first excited state can be explained analogously to the ground state of mixed valence compounds.

In Chart 1, four different D−π−D systems (hereafter called "dimers") with a conjugated bridge are displayed. They have been synthesized recently,[10−12] and their radical cations have been studied before.[11−13] Although **1** has a *p*-xylene bridge, this is replaced in **3** by anthracene, which has a smaller HOMO−LUMO gap. In compound **4** the dianisylamino groups are replaced by di(*p*-chlorophenyl)amino groups, which possess a higher oxidation potential and, thus, are somewhat weaker electron donors.[14] Systems containing anthracene as the bridge moiety attracted considerable attention in recent years because of their unusual properties in "molecular wire" systems.[15−22] The fourth system, **2**, has a formally broken π conjugation although it is well known that the [2.2]paracyclophane bridge includes a distinct direct orbital overlap between the π planes.[23−36] This effect was used in novel extended π systems for organic semiconductor applications.[37−49] For comparison with the D−π−D dimers we also include D-π reference systems **5** and **6** hereafter called "monomers". One aim of our investigation is to clarify whether the photophysical properties of **1**−**4** can be deduced from the monomeric reference systems or whether cooperative effects play a role, that is, whether the properties are additive (weak coupling of asymmetric subunits) or whether the coupling of subunits is strong. We will also address the problem of symmetry breaking, which plays an important role in the photophysics of these symmetric D−π−D systems particularly in polar solvent environments.[50−59]

Methods

Experimental Section. Absorption spectra were measured in spectrograde solvents using a JASCO V570 spectrometer with 2 nm resolution. Fluorescence spectra were recorded at very low concentrations ($c < 2 \times 10^{-6}$) in degassed spectrograde solvents and corrected for the wavelength dependence of the detector sensitivity using a PTI QuantaMaster Model QM-2000-4 spectrometer. The fluorescence quantum yield was determined relative to Rhodamine 101.[60] The fluorescence lifetime was determined using a PTI TimeMaster TM-2/2003 spectrometer with a flash lamp charged with a 1:1 H_2/N_2 mixture. The instrument response function (ca. 2.1 ns) was measured by a Ludox scatterer. For excitation energy we employed the N_2 band at 358 nm. The fluorescence decay was single-exponential in all cases; the quality of the fit was judged by the χ^2 values, the Durbin−Wattson parameter, the autocorrelation function, and the residuals.

* Corresponding authors. E-mail: lambert@chemie.uni-wuerzburg.de; ingo@phys-chemie.uni-wuerzburg.de.
† Institut für Organische Chemie.
‡ Institut für Physikalische Chemie.

10.1021/jp056728p CCC: $33.50
Published on Web 03/30/2006

CHART 1

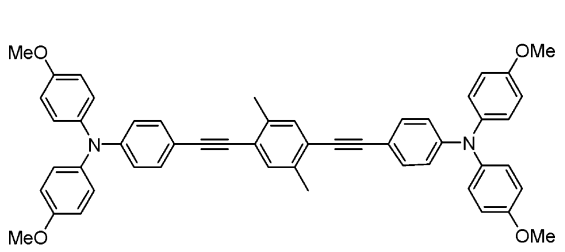

1

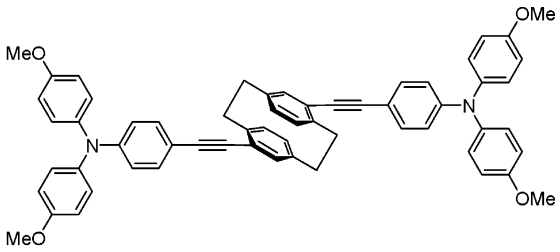

2

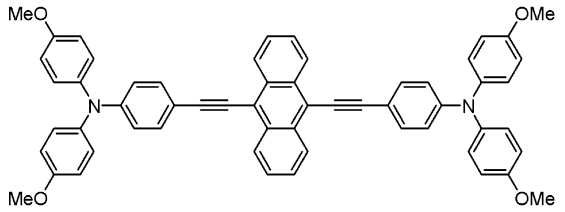

3

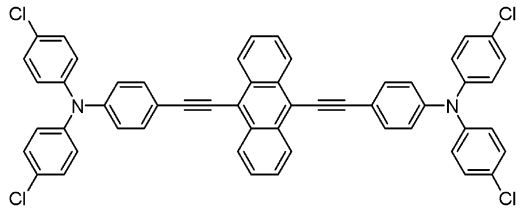

4

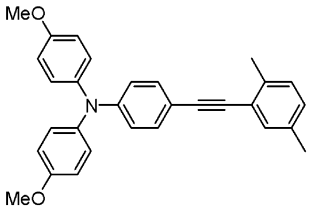

5

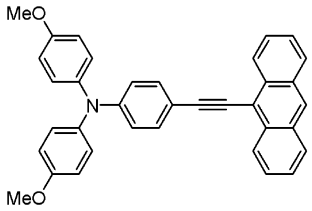

6

The experimental setup of the picosecond time-resolved transient absorption measurement is similar to the one published in refs 61 and 62. For sample excitation either the second (3−5 mJ) or third (1 mJ) harmonic of a mode-locked Nd:YAG laser (Continuum PY61C-10) was used. A white-light probe beam was generated by focusing the Nd:YAG laser fundamental at 1064 nm into a D_2O filled cell. The white-light continuum was split in two parts that were directed into the sample cell by quartz fibers at an angle of 90° with respect to the excitation beam. One part served as the reference beam, the other one was overlapped with the pump beam. The two white-light beams were further directed by fibers into a spectrograph with a diode array for spectral analysis. The delay time between the pump beam and the white-light probe beam was adjusted by a computer-controlled motorized delay stage. Each data point (i.e., a complete spectrum at each time delay) usually consists of an average of 100 shots. Although concentrations were varied, typically between 5×10^{-5} mol/L and 1×10^{-4} mol/L were employed. Measurements of β carotene in $C_2H_4Cl_2$ were used to derive the zero in time as well as the instrument response function (fwhm = 35−40 ps).

Data Evaluation. Because the origin transition is not accurately discernible in all experimental absorption and fluorescence spectra, we calculate the averaged reduced absorption and fluorescence energy, respectively, which are given in eq 1 and 2 where I_f is the fluorescence intensity versus wavenumber.[63] These reduced energies deviate from the apparent absorption and fluorescence maxima $\tilde{\nu}_{abs-max}$ and $\tilde{\nu}_{fl-max}$, respectively.

$$\tilde{\nu}_{abs} = \int \epsilon \, d\tilde{\nu} / \int \epsilon \, \tilde{\nu}^{-1} \, d\tilde{\nu} \tag{1}$$

$$\tilde{\nu}_{fl} = \int \tilde{\nu}^{-2} I_f \, d\tilde{\nu} / \int \tilde{\nu}^{-3} I_f \, d\tilde{\nu} \tag{2}$$

The transition moment, μ_{abs}, for the absorption process is obtained from eq 3 where n is the index of refraction of the solvent and the integration has to be performed over the reduced absorption spectrum.[63,64]

$$\mu_{abs}^2 = \frac{3hc\epsilon_0 \ln 10}{2000\pi^2 N} \frac{9n}{(n^2+2)^2} \int \frac{\epsilon}{\tilde{\nu}} d\tilde{\nu} \tag{3}$$

The oscillator strength was calculated as

$$f_{abs,fl} = \frac{8\pi^2 m_e c \tilde{\nu}_{abs,fl}}{3he^2} \mu_{abs,fl}^2 \tag{4}$$

where μ is the transition moment for absorption or fluorescence, respectively.[63]

If there is no drastic change of the electronic and geometric character of the excited state during its lifetime, then the transition moment for the absorption (μ_{abs}) and fluorescence (μ_{fl}) should be equal. The fluorescence transition moment, μ_{fl}, can be evaluated by the Strickler−Berg relation (eq 5) where the averaged cubic fluorescence energy (eq 6) is used and g_e and g_g are the degree of degeneracy of the ground and excited state.[65]

$$k_f = \frac{16 \times 10^6 \pi^3}{3h\epsilon_0} \frac{n(n^2+2)^2}{9} \frac{g_g}{g_e} \langle \tilde{\nu}_{fl}^{-3} \rangle_{av}^{-1} \mu_{fl}^2 \tag{5}$$

$$\text{with } \langle \tilde{\nu}_{fl}^{-3} \rangle_{av}^{-1} = \int I_f \, d\tilde{\nu} / \int \tilde{\nu}^{-3} I_f \, d\tilde{\nu} \tag{6}$$

The fluorescence rate constant, k_f, was determined experimentally from the fluorescence quantum yield, Φ, and the fluorescence lifetime, τ, by $k_f = \Phi/\tau$. The rate constant for nonradiative processes was calculated by $k_{nr} = (1/\tau) - k_f$.[63]

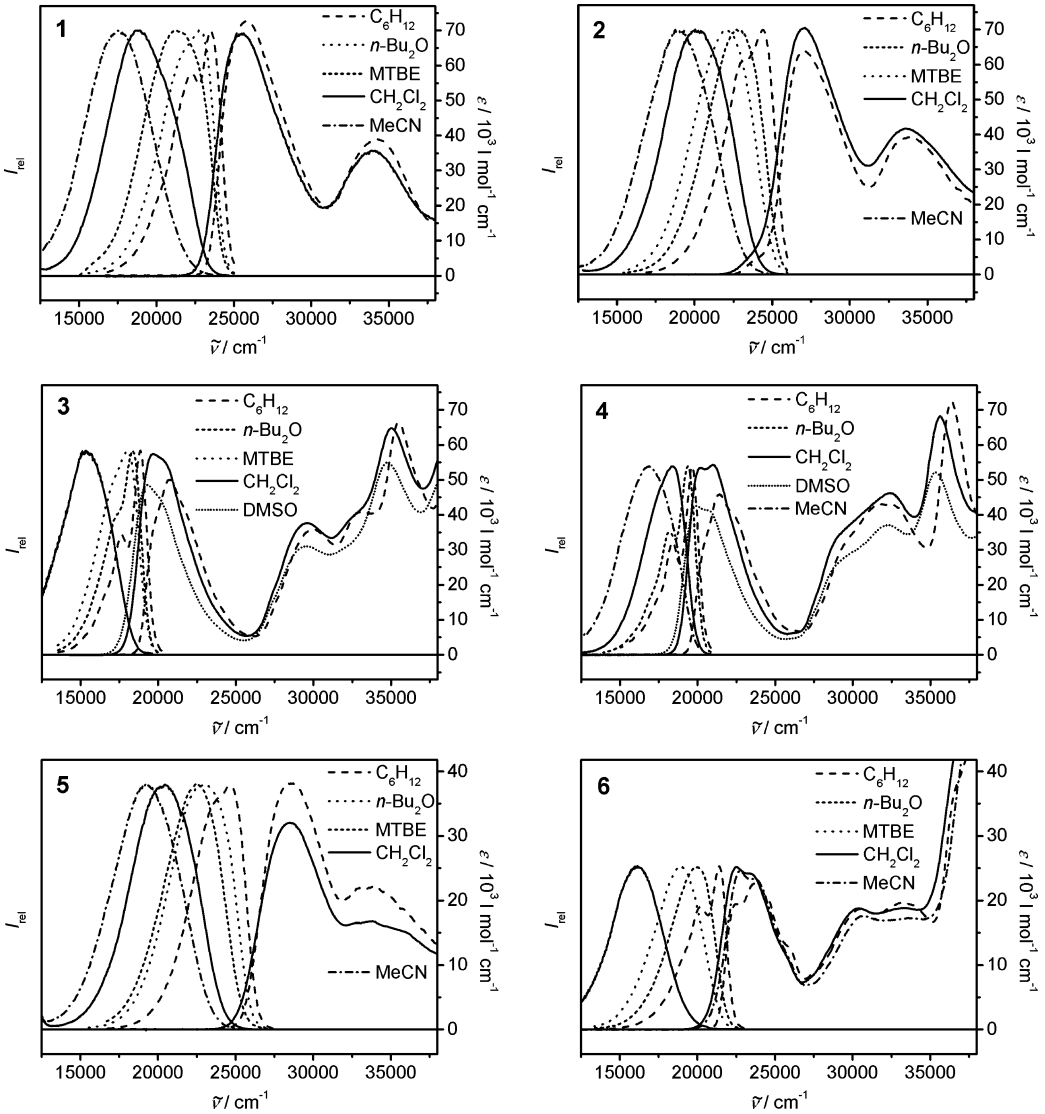

Figure 1. Absorption and fluorescence spectra of **1**−**6** in selected solvents.

In a purely classical model with parabolic ground and excited-state potentials for a combined solvent and molecular mode the free energy difference ΔG^{00}_{class} between the ground and excited state can be calculated by eq 7 and the total reorganization for the absorption and fluorescence process energy $\lambda_{class} = \lambda_v + \lambda_o$ is given by eq 8.

$$\Delta G^{00}_{class} = \frac{\tilde{\nu}_{abs} + \tilde{\nu}_{fl}}{2} \tag{7}$$

$$\lambda_{class} = \lambda_v + \lambda_o = \frac{\tilde{\nu}_{abs} - \tilde{\nu}_{fl}}{2} \tag{8}$$

The dipole moment differences between the ground and excited state was estimated by the method of Lippert and Mataga (eq 9) using a plot of the Stokes shift versus the Onsager solvent parameter.[66,67]

$$\tilde{\nu}_{abs} - \tilde{\nu}_{fl} = \frac{(\vec{\mu}_e - \vec{\mu}_g)^2}{2\pi\epsilon_0 hc a_0^3}(f(\epsilon) - f(n^2)) + (\tilde{\nu}^{gas}_{abs} - \tilde{\nu}^{gas}_{fl}) \tag{9}$$

$$\text{with } f(\epsilon) = \frac{\epsilon - 1}{2\epsilon + 1} \text{ and } f(n^2) = \frac{n^2 - 1}{2n^2 + 1}$$

where μ_e and μ_g are the excited and ground-state dipole moments, respectively. The *y*-axis intercept corresponds to $(\tilde{\nu}^{gas}_{abs} - \tilde{\nu}^{gas}_{fl})$, and the slope of the plot yields the dipole-moment difference.

Results

Stationary Spectroscopy. The absorption and fluorescence spectra of **1**−**6** are given in Figure 1. All compounds show a distinct low energy absorption, which in the cases of **3** and **4** is well separated from higher-energy bands. For anthracene compounds **3**, **4**, and **6** this band appears at distinctly lower energy than in the other compounds, which is due to a stronger CT character of this transition owing to the stronger acceptor properties of anthracene. In the absorption spectra of anthracene compounds **3**, **4**, and **6** some vibronic structure is discernible in both apolar and polar solvents. It is immediately obvious that while the absorption spectra are only slightly solvent-dependent, the fluorescence spectra show a pronounced bathochromic solvatochromism. Thus, all compounds show strong Stokes shifts in polar solvents.

The width of the fluorescence signals, $\Delta\tilde{\nu}_{1/2}$, is significantly narrower for both anthracene dimers **3** and **4** (e.g., for **4** in C_6H_{12} $\Delta\tilde{\nu}_{1/2} = 2000$ cm^{-1}) in comparison to that of dimers **1** and **2** (e.g., for **2** in C_6H_{12} $\Delta\tilde{\nu}_{1/2} = 3500$ cm^{-1}). Furthermore, in

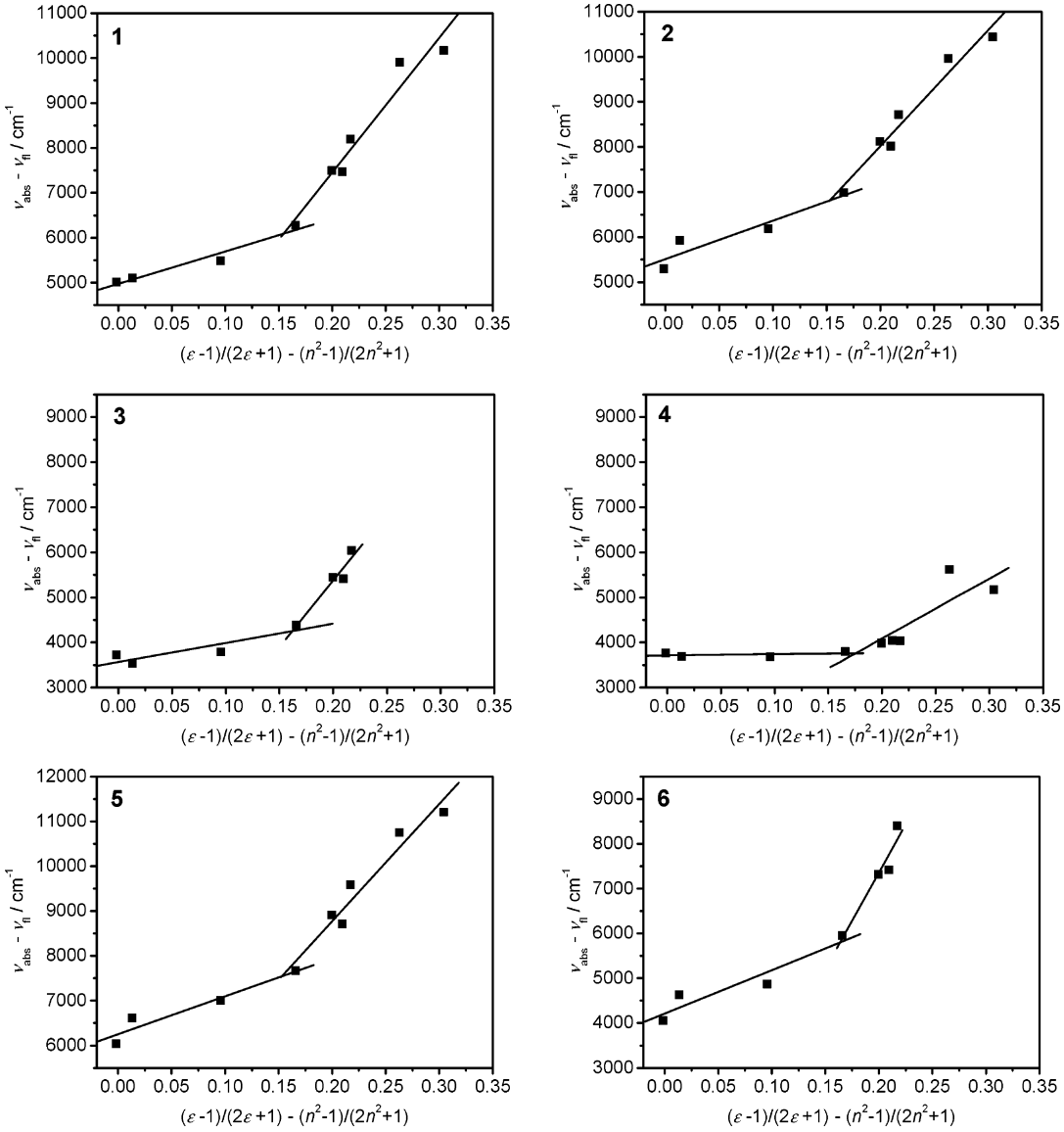

Figure 2. Lippert−Mataga plots for **1**−**6**, yielding the dipole moment difference, $\Delta\mu$, from the slopes. The solvents are (from left to right) C_6H_{12}, toluene, *n*-Bu_2O, MTBE, EtOAc, THF, CH_2Cl_2, DMSO, and MeCN.

CH_2Cl_2 the fluorescence signal of **3** ($\Delta\tilde{\nu}_{1/2}$ = 3900 cm^{-1}) is much broader than that of **4** ($\Delta\tilde{\nu}_{1/2}$ = 3000 cm^{-1}). These narrow bandwidths of anthracene **3**, particularly in apolar media, and the small bandwidths of **4** in the whole polarity range indicate delocalized first excited states.

The fluorescence spectra of all compounds also display vibronic structure in apolar solvents, whereas they are completely diffuse in the more polar solvents. For the symmetric anthracene containing species **3** and **4** the vibrational structure is most pronounced in cyclohexane and more recognizable than in the asymmetric analogue **6**. An exact mirror relationship of reduced absorption and fluorescence spectra was not observed in any case.

The transition moments for absorption, μ_{abs}, and the related oscillator strength, f_{abs}, were calculated by eqs 3 and 4. Symmetric D−π−D compounds **1**, **2**, and **3** have oscillator strengths twice as high as their asymmetric analogues **5** and **6**, respectively.

The total reorganization energy, λ_{class}, for the absorption and fluorescence process was calculated by eq 8. It increases strongly on going from apolar to polar solvents for all compounds. However, this effect is less pronounced for anthracene compounds **3** and **4**. The free energy difference between the relaxed excited state and the relaxed ground state was calculated by eq 7. This free energy difference decreases with increasing solvent polarity. Both trends, for λ_{class} and for ΔG^{00}_{class}, cancel out for the absorption but add for the fluorescence process, which explains the different solvatochromic behavior.

The Lippert−Mataga plots of $\tilde{\nu}_{abs} - \tilde{\nu}_{fl}$ versus the Onsager solvent parameter (Figure 2) shows distinct differences for nonpolar and polar solvents; that is, for the weakly polar solvents a linear correlation with small slope is observed, whereas for polar solvents a much steeper slope is found. From the differences of slopes it is evident that the dipole moment differences are small in apolar solvents and much higher in the set of polar solvents. This behavior indicates a major molecular reorganization in the excited state in polar solvents. Compound **4** exhibits a relatively small dipole moment change, $\Delta\mu$, indicating less charge separation than in the other compounds. The solute radii, a_0, were estimated as one-fourth of the maximum molecular dimension of the dimers, which was obtained from the AM1 optimized dimer structures. For monomers **5** and **6** the radii derived from corresponding dimers **1** and **3** were used to calculate the dipole moment differences

TABLE 1: Dipole Moment Differences of 1−6 (Nonpolar/Polar) Estimated by the Method of Lippert−Mataga (Eq 9)

	1	2	3	4	5	6
a_0 (10^{-10}m)	7.61	7.83	7.60	6.82	7.61	7.60
$\Delta\mu$ (D)	17.8/36.2	20.1/35.0	13.6/35.8	3.0/20.4	19.2/33.8	20.5/43.2

between the excited and the ground state in both sets of solvents (see Table 1).

Time-Resolved Fluorescence Spectroscopy. Fluorescence quantum yields, ϕ, are generally high for all compounds (see Table 2 and Table 3). However, there are significant differences between the symmetric D−π−D compounds and the corresponding reference compounds (monomers): Both the species with *p*-xylene (**1**) and the paracyclophane bridge (**2**) show distinctly higher quantum yields than **5** in most solvents. Much in contrast, anthracene compound **3** has a lower quantum yield than **6**. The quantum yields of the latter, like those of **4**, approach unity in most solvents.

The fluorescence lifetimes of all compounds are between ca. 1 and 5 ns. Even for the anthracene-containing species the lifetime is only 2−3 ns in apolar solvents, which demonstrates that there is a mixing of anthracene excited states with states of the other molecular parts because pure anthracene itself has a longer lifetime (5.2 ns in cyclohexane).[68] We note that 9,10-bis(phenylethynyl)anthracene also has a shorter fluorescence lifetime than anthracene in apolar media (3.2 ns).[69]

For cyclophanes like **2** a "phane" state is frequently discussed in the literature, which is the first excited state of pseudo-*p*-[2.2]paracyclophane with small substituents.[26,29] These states are generally characterized by relatively long lifetimes. However, the electronic situation is different for larger substituents as in our case for [2.2]paracyclophane **2**, which might explain the smaller fluorescence lifetimes.

From the fluorescence rate constants we calculated the fluorescence transition moment, μ_{fl}, by eq 5 and the oscillator strength by eq 4. Similar to the absorption oscillator strength, f_{abs} (see Tables 2 and 3), the fluorescence oscillator strength for **2** is twice as high as that of its asymmetric analogue, **5**. However, compounds **1** and **3** show a different behavior: Although f_{fl} of **1** is three to four times as high as f_{fl} of **5**, that of **3** is about the same as that of **6**. This fact points toward nonadditive effects (strong interactions) in the chromophore branches in the excited states of **1** and of **3**.

Picosecond Time-Resolved Transient Absorption Spectroscopy. The picosecond time-resolved transient absorption spectra of compounds **1**−**6** were recorded in apolar toluene as well as in the polar solvent benzonitrile (PhCN). A solvent-dependent investigation of the excited-state dynamics of compounds **1**−**6** is of interest because the Lippert−Mataga plots already indicate that for all compounds the nature of the first excited state depends on the solvent polarity. In most experiments the samples were excited with a pump wavelength of 355 nm (28 200 cm^{-1}), with the exception of **3** in toluene and **4** in toluene and PhCN, which were excited at 532 nm (18 800 cm^{-1}). The spectra are given in Figure 3. In all graphs the dashed line corresponds to a spectrum recorded before the zero in time, that is, a background spectrum, the solid line corresponds to a spectrum at maximum signal, approximately around the zero in time, and the dotted line corresponds to a spectrum recorded at longer delay times. Beside the transient absorption bands negative absorption due to ground-state bleaching or steady-state emission caused by the excitation laser is visible in some experiments. The most important spectral features of compounds **1**−**6** in the transient absorption spectra recorded around time zero (see Figure 3) are summarized in Table 4.

All molecules show an intense absorption band between 13 000 and 15 000 cm^{-1}. Such a band is typical of triarylamine radical cations.[14] For example, in the transient absorption of neutral diansiylphenylamine a signal around 14 500 cm^{-1} was observed.[70] In the same energy region a transient absorption was also found for acridine-triarylamine donor−acceptor compounds,[70] acridine−triarylamine redox cascades[70] and neutral triarylmethyl−triarylamine mixed-valence compounds.[71] The presence of this $\pi-\pi^*$ band typical of triarylamine radical cations in the spectra of all compounds indicates formation of a charge-separated excited CT state in both solvents. In fact, absorptions in this region are visible in the spectra of all compounds in both solvents. The positive solvatochromism observed for the corresponding transitions in compounds **2**, **4**, and **5** supports this assignment.[14]

On the basis of the Lippert−Mataga plots, we expect a charge-separated excited CT state for *p*-xylenes **1** and **5** and [2.2]paracyclophane **2** and, therefore beside the absorption typical of the triarylamine radical cation, we expect to see another absorption due to the radical anion of the corresponding bridge acceptor. The unsubstituted [2.2]paracyclophane radical anion itself shows one absorption band at 12 200 cm^{-1} and a second at 26 000 cm^{-1} in MTHF,[72] whereas the unsubstituted benzene radical anion is characterized by only one band at ca. 26 000 cm^{-1} in MTHF.[73] Because the conjugating substitutents in excited *p*-xylenes **1** and **5** may shift the *p*-xylene anion absorption band to smaller wavenumbers, we suppose that the absorptions of **1** and **5** above 16 000 cm^{-1} can be traced back to this *p*-xylene radical anion absorption. In contrast, cyclophane **2** does not show the typical absorption bands of the [2.2]-paracyclophane radical anion at 12 200 and 26 000 cm^{-1} (the latter might be hidden by strong emission in toluene).[72] This might also be due to the fact that the substituents at the cyclophane moiety shift both bands significantly to the red and, thus, the absorption bands of **2** at 18 500 cm^{-1} in toluene and 20 000 cm^{-1} in PhCN are the corresponding radical anion bands. Interestingly, the transient absorption of donor-substituted paracyclophane **2** shows significant differences compared to the transient absorption of pseudo-*p*-distyryl-[2.2]paracyclophane.[74] Dimer **2** shows two maxima, whereas pseudo-*p*-distyryl-[2.2]-paracyclophane shows an intense and broad but featureless transient absorption between 8000 and 22 000 cm^{-1}.[74] This indicates that the triarylamine donor groups have significant influence on the nature of the excited states. We suppose that the different absorption properties can be explained by a delocalized first excited state without charge separation of pseudo-*p*-distyryl-[2.2]paracyclophane while a charge separated excited CT state of D−π−D compound **2** is observed. *p*-Xylene **1** shows a broad transient absorption in both solvents, which has three maxima in toluene but only a shoulder on the high energy side in PhCN. We assume that the absorption of **1** is the result of at least two electronic transitions. On one hand we observe the *p*-xylene radical anion band at wavenumbers larger than ~16 000 cm^{-1}, and on the other hand there is a triarylamine excited-state absorption at 13 500 cm^{-1} (toluene) and 14 000 cm^{-1} (PhCN), respectively.

Comparison of the transient absorption spectra in toluene and PhCN shows for all compounds with the exception of **4** significant differences of the absorption properties upon changing the solvent polarity. In toluene, the first excited state of anthracenes **3**, **4**, and **6** shows an absorption at low energy between 10 500 and 11 500 cm^{-1}. The remaining compounds with either a *p*-xylene bridge (**1** and **5**) or the [2.2]paracyclophane bridge (**2**) do not show any transient absorption below

TABLE 2: Linear Optical Properties of 1, 2, and 5

	$\tilde{\nu}_{abs}$ (cm^{-1})	μ_{abs} (D)	f_{abs}	$\tilde{\nu}_{fl}$ (cm^{-1})	ϕ	τ_{fl} (ns)	k_f (ns^{-1})	k_{nr} (ns^{-1})	μ_{fl} (D)	f_{fl}	λ_{class} (cm^{-1})	ΔG^{00}_{class} (cm^{-1})
1												
C_6H_{12}	26 860	9.3	1.09	21 860	0.81	0.8	1.03	0.24	10.9	1.22	2510	24 360
toluene	26 350	9.1	1.03	21 240	0.80						2550	23 790
n-Bu_2O	26 670	9.8	1.20	21 190	0.93	1.2	0.79	0.06	10.3	1.06	2740	23 930
MTBE	26 690	10.5	1.38	20 420	0.82	1.5	0.55	0.12	9.4	0.85	3140	23 560
EtOAc	26 590	9.7	1.18	19 100	0.65						3750	22 840
THF	26 510	9.9	1.22	19 040	0.87	2.2	0.40	0.06	8.5	0.65	3740	22 780
CH_2Cl_2	26 400	9.7	1.17	18 220	0.70	2.7	0.26	0.11	7.3	0.46	4100	22 310
DMSO	26 210			16 310	0.33						4950	21 260
MeCN	26 650	10.5	1.38	16 480	0.36	1.4	0.25	0.45	8.9	0.61	5090	21 570
2												
C_6H_{12}	28 040	8.8	1.02	22 750	0.52	1.1	0.48	0.44	7.0	0.52	2650	25 390
toluene	27 590	9.1	1.07	21 670	0.71						2960	24 630
n-Bu_2O	27 900	9.6	1.21	21 710	0.72	1.7	0.44	0.17	7.4	0.56	3090	24 800
MTBE	27 980	9.9	1.29	21 000	0.63	1.7	0.38	0.22	7.5	0.56	3490	24 490
EtOAc	28 090	10.6	1.48	19 970	0.70						4060	24 030
THF	27 900	9.5	1.18	19 880	0.91	3.3	0.27	0.03	6.6	0.41	4010	23 890
CH_2Cl_2	28 030	9.8	1.27	19 320	0.92	4.0	0.23	0.02	6.2	0.35	4360	23 680
DMSO	27 910	9.5	1.18	17 960	0.76						4980	22 930
MeCN	28 480	9.9	1.31	18 050	0.77	3.7	0.22	0.06	7.1	0.43	5220	23 270
5												
C_6H_{12}	29 220	6.9	0.65	23 180	0.35	1.1	0.32	0.60	5.6	0.34	3020	26 200
toluene	28 810	6.3	0.54	22 200	0.44						3310	25 500
n-Bu_2O	29 000	6.3	0.54	21 990	0.39	1.5	0.26	0.41	5.6	0.32	3500	25 490
MTBE	29 140	6.1	0.51	21 480	0.58	2.7	0.21	0.15	5.4	0.29	3830	25 310
EtOAc	29 200	6.8	0.63	20 300	0.50						4450	24 750
THF	29 030	6.9	0.65	20 310	0.70	3.9	0.18	0.08	5.2	0.26	4360	24 670
CH_2Cl_2	29 090	6.5	0.58	19 510	0.71	5.0	0.14	0.06	4.8	0.21	4790	24 300
DMSO	28 960	6.5	0.58	18 210	0.75						5380	23 590
MeCN	29 470	6.7	0.62	18 260	0.46	5.0	0.09	0.11	4.6	0.18	5600	23 870

TABLE 3: Linear Optical Properties of 3, 4, and 6

	$\tilde{\nu}_{abs}$ (cm^{-1})	μ_{abs} (D)	f_{abs}	$\tilde{\nu}_{fl}$ (cm^{-1})	ϕ	τ_{fl} (ns)	k_f (ns^{-1})	k_{nr} (ns^{-1})	μ_{fl} (D)	f_{fl}	λ_{class} (cm^{-1})	ΔG^{00}_{class} (cm^{-1})
3												
C_6H_{12}	21 370	7.3	0.54	17 650	0.74	2.4	0.31	0.11	8.2	0.56	1860	19 510
toluene	20 770	8.4	0.69	17240	0.78						1760	19 000
n-Bu_2O	21 000	6.8	0.46	17 210	0.80	2.0	0.40	0.10	10.1	0.83	1890	19 100
MTBE	21 230	7.5	0.56	16 850	0.84	3.2	0.27	0.05	8.7	0.60	2190	19 040
EtOAc	21 130	8.8	0.77	15 690	0.52						2720	18 410
THF	20 830	8.7	0.74	15 420	0.47	3.2	0.15	0.17	7.1	0.37	2700	18 130
CH_2Cl_2	20 640	8.6	0.72	14 590	0.31	2.3	0.14	0.30	7.3	0.37	3020	17 610
DMSO	20 230	7.8	0.58									
MeCN						0.9						
4												
C_6H_{12}	22 140	7.3	0.55	18 380	0.94	2.4	0.40	0.03	8.8	0.67	1880	20 260
toluene	21 580	7.7	0.60	17 890	1.00						1840	19 740
n-Bu_2O	21 810	8.0	0.66	18 130	1.00	2.8	0.36	0.00	8.8	0.66	1840	19 970
MTBE	21 910	8.5	0.74	18 110	1.00	2.6	0.39	0.00	9.4	0.75	1900	20 010
EtOAc	21 670	8.8	0.79	17 690	0.89						1990	19 680
THF	21 570	8.5	0.73	17 520	1.00	2.5	0.41	0.00	9.7	0.78	2020	19 550
CH_2Cl_2	21 410	8.3	0.69	17 380	1.00	2.6	0.38	0.00	9.5	0.74	2020	19 390
DMSO	21 080	7.2	0.51	15 470	0.83						2810	18 280
MeCN	21 170			16 000	0.78	3.2	0.24	0.07	9.1	0.62	2580	18 580
6												
C_6H_{12}	23 960	5.3	0.32	19 910	0.97	2.6	0.37	0.01	9.0	0.76	2030	21 930
toluene	23 600	5.7	0.36	18 970	0.99						2310	21 290
n-Bu_2O	23 800	5.6	0.35	18 930	0.96	3.1	0.31	0.01	8.9	0.70	2440	21 360
MTBE	23 960	5.7	0.37	18 010	0.89	3.4	0.26	0.03	8.7	0.64	2980	20 980
EtOAc	23 810	5.7	0.36	16 490	0.73						3660	20 150
THF	23 680	5.7	0.36	16 270	0.82	5.1	0.16	0.04	7.4	0.42	3710	19 970
CH_2Cl_2	23 650	5.7	0.36	15 250	0.54	4.5	0.12	0.10	6.8	0.33	4200	19 450
DMSO	23 960											
MeCN	23 600	5.7	0.36			0.2						

13 500 cm^{-1} neither in toluene nor in PhCN. This indicates that this absorption at low energy is due to a transition closely related to the anthracene bridge itself.[75−79] From the Lippert−Mataga plots (Figure 2), a charge-separated CT state is expected only for anthracenes **3** and **6**. These CT states should be characterized by a partial positive charge on the triarylamine moiety and a partial negative charge on the anthracene bridge. Although, as judged from the Lippert−Mataga plots in Figure 2, the CT character is less pronounced for the chloro-substituted anthracene bridged compound, **4**, and the absorption bands for all anthracenes in toluene are very similar. Even compound **4** shows the characteristic triarylamine radical cation $\pi-\pi^*$ band.

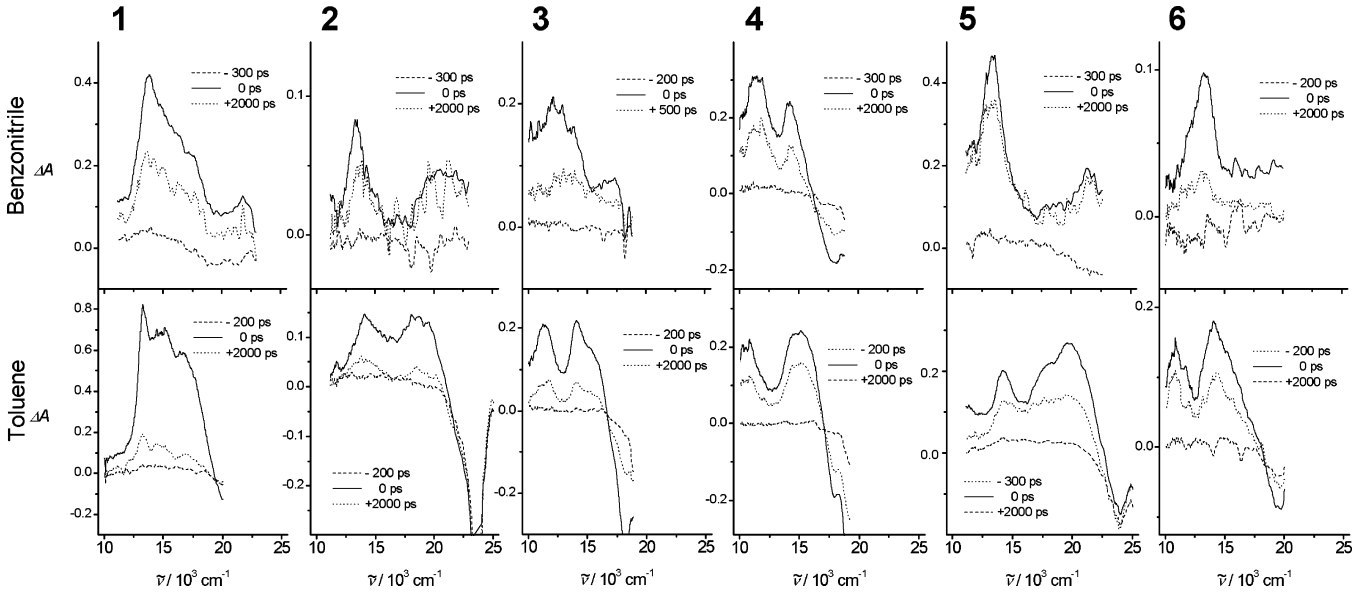

Figure 3. Transient absorption spectra of **1**−**6** in benzonitrile (upper trace) and toluene (lower trace).

TABLE 4: Transient Absorption Maxima of 1−6 in cm^{-1} (sh = shoulder, br = broad) and Lifetimes τ in ns

	1	**2**	**3**	**4**	**5**	**6**
PhCN	14 000 (br)	13 500	10 000	11 500	13 500	12 000 (sh)
	16 000 (sh)	22 000	14 500	14 000	18 500 (sh)	13 500
	22 000		17 000	18 000 (bleach)	21 500	
τ (ns)	2.8	3.4	0.5	2.4	4.5	1.5
toluene	13 500	14 000	11 500	10 500	14 500	11 000
	15 000	18 500	14 000	15 000	17 500 (sh)	14 000
	16 500		15 500 (sh)		19 500	
	>20 000 (bleach)	23 000 (emission)	18 000 (bleach)	18 500 (bleach)	24 000 (emission)	19 500 (em/bleach)
τ (ns)	1.2	1.5	2.0	2.5	2.4	3.2

This observation reflects that the degree of charge separation does not significantly influence the absorption caused by a triarylamine moiety. A similar conclusion has been drawn recently for acridine−triarylamine redox cascades.[70] However, the transient absorption spectra show a more pronounced influence of the solvent polarity for compounds **3** and **6** than for **4**. We suppose that this fact is a consequence of the distinctly more delocalized first excited state of **4**. The signals of **4** and **6** at smaller wavenumbers (10 000−12 000 cm^{-1}, related to the anthracene bridge anion) show negative solvatochromism, whereras the signals of **4** and **6** at higher energy (13 000−15 000 cm^{-1}, related to the triarylamine cation) show positive solvatochromism. This assumes that the low energy band of **6** in toluene corresponds to the shoulder at 12 000 cm^{-1} of the main peak in PhCN. In contrast, a more pronounced effect of the solvent polarity on the transient absorption was found for anthracene **3**, which shows a very broad and featureless transient absorption in PhCN between 10 000 and 14 500 cm^{-1} and an additional weak absorption at 17 000 cm^{-1}.

With exception of **3** in PhCN (τ = 500 ps), lifetimes on the order of a few ns were observed (Table 4). Similar decay times were derived for all spectral features (absorption bands and ground-state bleach) in a given spectrum. Within the experimental error they are in good agreement with the fluorescence lifetimes (Tables 2 and 3) in nonpolar media and polar solvents, respectively.

Several transient spectra show additional negative absorptions. In all spectra recorded with an excitation at 532 nm (**3** and **4** in toluene, **4** in PhCN), as well as the spectrum of **1** in toluene, a signal is visible that can be assigned to a ground-state bleach. The similar time constant for ground-state recovery and absorption decay confirm that the excited-state decay is due to a return to the electronic ground state with no additional intermediate state. However, in compounds **2** and **5** the negative absorption in toluene is due to a probe-independent emission caused by the excitation laser. At least in compound **6** it seems that such an emission conceals an additionally present ground-state bleach.

Discussion

For the interpretation of the photophysical properties of the D−π−D compounds we construct the ground and excited state adiabatic potential energy surfaces (PES) by mixing three diabatic (formally noninteracting) states in a two-mode approximation (one asymmetric (x) and one symmetric mode (y)). A similar model was already used for the description of the PESs of analogous ground-state mixed-valence radical cations.[11−13] The three diabatic states are the ground state and two degenerate excited CT states.[80] In the latter the excitation is localized in one-half of the D−π−D chromophore, (D$^+$−π^- −D) or (D−π^- −D$^+$), respectively (see Figure 4).

These two degenerate CT states have local CT character as indicated by the solvatochromism of the fluorescence (see above). Coupling of these two excited diabatic states yields the two excited states S_1 and S_2. For the excited-state electronic coupling, V, we use half of the energy splitting between the S_1 and the S_2 states as determined by two-photon absorption (TPA) measurements (Table 5).[10] The couplings between the ground and the two degenerate excited CT states are neglected (V_{12} = V_{23} = 0 cm^{-1}) in this model.

We used the above evaluated electronic couplings and harmonic potentials with reorganization energies λ for construct-

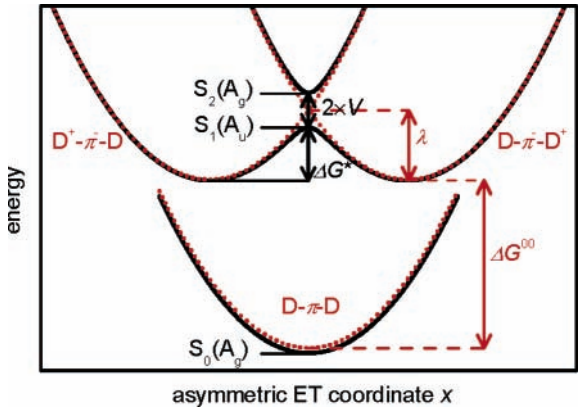

Figure 4. One-dimensional projection of diabatic (red, dotted line) and adiabatic PES (black, full line) of a D−π−D excited state mixed-valence system.

TABLE 5: S_1−S_2 Splitting and Electronic Couplings from Two-Photon Absorption Measurements[10] in cm^{-1}

	1	**2**	**3**	**4**
S_2(TPA)−S_1	2300	480	3400	3600
V	1200	240	1700	1800

ing the adiabatic PES. The minima of the three diabatic potentials are chosen in a way that they form a regular triangle on a two-dimensional potential map (x, y coordinates). We employ dimensionless reaction coordinates connecting the three states. The distance between these states is set to unity on the x, y potential map.

Diagonalization of matrix 10 yields the adiabatic PES with the three states S_0, S_1, and S_2 (see Figure 5). If we assume C_i symmetry to be the highest symmetry in compounds **1**−**4**, then the electronic state S_0 possesses A_g symmetry, S_1 is A_u symmetric, and S_2 has again A_g symmetry. The reorganization energies, λ, as well as the free energy difference, ΔG^{00}, between the diabatic ground state and the diabatic degenerate excited states were optimized in order to reproduce the experimentally observed absorption and fluorescence energies as indicated by yellow arrows in Figure 5. The resulting ΔG^{00} and λ (see Table 6) are all somewhat larger than ΔG^{00}_{class} and λ_{class} (see Tables 2 and 3), respectively. The deviations are significant for the strongly coupled anthracene dimers **3** and **4**, medium for *p*-xylene **1**, and small for the weakly coupled paracyclophane **2**. However, taking into account the semiempirical character of our model and the approximations implicit in eqs 7 and 8, the agreement of the resulting λ, ΔG^{00} with λ_{class} and ΔG^{00}_{class} is considered to be reasonable.

In the following we will interpret the photophysical processes in the symmetrical *p*-xylene **1** using the three-level approximation described above. Dimer **1** can formally be divided into two **5** subunits that are electronically coupled: Excitation of **1** yields an initially symmetrical excited Franck−Condon state as indicated by the lack of solvatochromism in the absorption process. This Franck−Condon state is at the ridge between two minima. The transition into the S_1 state is symmetry allowed, whereas the transition into the S_2 state is one-photon forbidden and only allowed in a two-photon process, see ref 10. As evident from Figure 5, the S_1 state is distorted by a pseudo-Jahn−Teller-type effect.[81] It relaxes into one of two minima, which represent a symmetry-broken locally excited CT state in which a partial positive charge is localized on the triarylamine donor and the negative charge on the π bridge. From this symmetry-broken CT state, the molecule might return to the ground state by fluorescence. The large excited-state geometry relaxation also explains the large Stokes shifts as well as the broad fluorescence signals.

On the excited-state potential energy surface, the optical excitation from the relaxed S_1 state to a Franck−Condon S_2 state can be viewed as an excited-state intervalence charge transfer (cyan arrow in Figure 5) because in the diabatic limit it refers to the transfer of a positive charge from one triarylamine over the negatively charged π bridge to the other triarylamine moiety ($D^+-\pi^--D \rightarrow D-\pi^--D^+$). This excited-state intervalence charge transfer (IVCT) may in principle be observed in the transient absorption spectra of compounds **1**−**4**. The energy of this excited IVCT transition $S_2-S_1^{trans}$ (Table 6) was estimated from the adiabatic PES to lie between 2570 and 5660 cm^{-1} for all compounds. In fact, such an excited IVCT absorption was found, for example, for a bis-ruthenium tetracation $Ru^{II}-Ru^{II}$ at 6300 cm^{-1}.[82] Unfortunately, this energy is too low to be measurable in our present experimental setup.

For the weakly coupled paracyclophane, **2**, as well as *p*-xylene **1** the computed S_1 potential energy surface shows a double minimum potential in both apolar and polar media. This situation is reflected by the existence of a barrier along the x coordinate ΔG^* (which is y-coordinate independent) of the excited intervalence electron transfer (see Figure 5 for illustration) as estimated from the adiabatic PES (Table 6). Generally this barrier is large for weak coupling as well as for small solvent reorganization energy. In fact, only **1** and **2** have a CT barrier in both apolar and polar solvents. On the basis of the theoretical analysis, paracyclophane **2** shows the weakest coupling and, therefore, the adiabatic locally excited CT state at the minimum of the S_1 potential energy surface can be considered to be similar to the localized diabatic state ($D^+-\pi^--D$). Thus, this symmetry-broken diabatic state of paracyclophane **2** can be compared directly with the first excited state ($D^+-\pi^-$) of asymmetric subunit **5**. This close analogy explains that both the transient absorption spectra of **5** and **2** and the dipole moment differences, $\Delta\mu$, derived from the linear correlations in the Lippert−Mataga plots of **5** and **2** are very similar. Furthermore, the weak interactions of the subunits (diabatic states) in **2** are the reason for the additive behavior of the fluorescence oscillator strengths, f_{fl}. Because paracyclophane **2** is composed of two **5** subunits, the oscillator strengths, f_{fl}, of dimer **2** are approximately twice that of corresponding monomer **5** (see Table 2).

The stronger coupling of *p*-xylene dimer **1** has, in contrast to the weak coupling of **2**, a significant influence on the optical properties. This is demonstrated, in particular, by the nonadditive behavior of f_{fl}, which is three to four times as high as that for dimer **1** in comparison to f_{fl} of **5**. Interestingly, the fluorescence quantum yields, ϕ, of dimers **1** and **2** are larger than that of monomer **5** in most solvents. This cooperative effect of dimers **1** and **2** can be understood as an exciton superradiant

$$\begin{vmatrix} \lambda\left[\left(-\frac{1}{2}-x\right)^2+\left(\frac{\sqrt{3}}{2}-y\right)^2\right]+\Delta G^{00}-E & 0 & V \\ 0 & \lambda(x^2+y^2)-E & 0 \\ V & 0 & \lambda\left[\left(\frac{1}{2}-x\right)^2+\left(\frac{\sqrt{3}}{2}-y\right)^2\right]+\Delta G^{00}-E \end{vmatrix} = 0 \qquad (10)$$

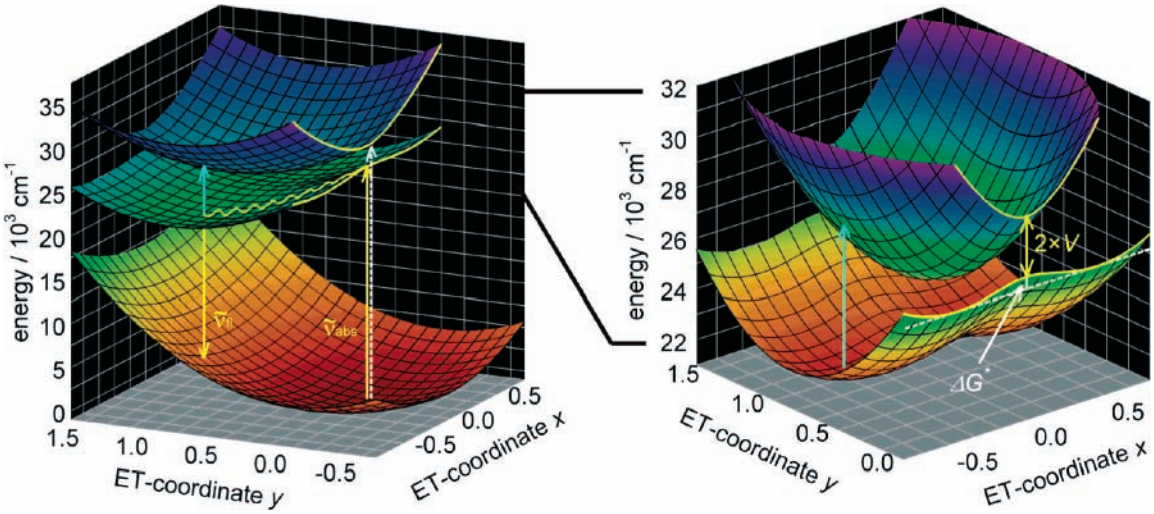

Figure 5. Adiabatic potential energy surfaces of **1** in MeCN (yellow arrows: absorption and fluorescence; dashed white arrow: two-photon absorption; cyan arrow: transient IVCT transition). The diagram on the right is a close-up of the S_1 and S_2 PES.

TABLE 6: Optimized ΔG^{00}, λ Values, Calculated ET Barriers, ΔG^*, and Transient IVCT Absorption Energies $S_2-S_1^{trans}$ in cm^{-1}

		λ	ΔG^{00}	ΔG^*	$S_2-S_1^{trans}$
1	C_6H_{12}	3100	24 950	40	3080
	MeCN	5700	22 150	480	5660
2	C_6H_{12}	2800	25 500	480	2570
	MeCN	5350	23 350	1110	4840
3	C_6H_{12}	2450	20 600	0	3400
	CH_2Cl_2	3900	18 450	20	3920
4	C_6H_{12}	2550	21 400	0	3600
	MeCN	3450	19 500	0	3600

emission:[83,84] In a weakly coupled dimer chromophore the absorption oscillator strength, f_{abs}, of the dimer is twice that of the monomer. Consequently, if there is no change in the nature of the excited-state transition moment, then the fluorescence oscillator strength, f_{fl}, of the dimer is twice that of the monomer. Because the fluorescence rate constant, k_f, is linearly correlated to the fluorescence oscillator strength, f_{fl} (see eqs 4 and 5) k_f of the dimer should be twice that of the monomer. The fluorescence quantum yield is given by $\phi = k_f/(k_f + k_{nr})$. Provided that $k_{nr} > k_f$ and the rate constant of nonradiative processes, k_{nr}, is constant it follows $\phi = k_f/k_{nr,const}$. Thus, it follows that the quantum yield of the dimer is also twice that of the monomer. Consequently, we interpret the significantly larger fluorescence quantum yields of dimers **1** and **2** compared to **5** as being due to an exciton superradiance of these dimers.

In contrast to **1** and **2**, the strongly coupled chloro-substituted anthracene, **4**, shows no CT barrier in either solvent ($\Delta G^* = 0$ cm^{-1}). Thus, the S_1 state is characterized by a single minimum potential. The excitation of **4** to the S_1 state is not followed by symmetry breaking because the S_1 state relaxes solely along the symmetric *y* coordinate to the symmetrically delocalized minimum. We suppose that the delocalized S_1 state of **4** explains the relatively weak solvent effect in both the absorption and fluorescence spectra as well as the similar appearance of the transient absorption spectra of anthracene **4** in both solvents. Furthermore, the comparably small dipole moment differences, $\Delta\mu$, derived from the Lippert−Mataga plots of **4** can be traced back to this delocalized character of the S_1 state. The single minimum potential of the S_1 state in apolar as well as polar media is also the explanation for the large and solvent-independent fluorescence quantum yields, ϕ, and the narrow bandwidth of the fluorescence signals because there is only along the symmetric coordinate *y* a significant reorganization in the first excited state of **4**. A consequence of the single minimum PES of the first excited state is that a possible intersection of the S_0 and S_1 potentials is localized at much higher energy and, therefore, the rate constant, k_{nr}, for nonradiative processes is small and the fluorescence quantum yield, ϕ, approaches unity.

The situation is different for the S_1 potential energy surface of methoxy-substituted anthracene **3**, which has a single minimum potential in a nonpolar medium but a double minimum potential with a small barrier in a polar solvent. Therefore, the fluorescence quantum yields of **3** are larger in apolar media than in polar media because there is no significant reorganization of the S_1 state in apolar medium as mentioned above (for anthracene **4**). Because the shape of the excited-state S_1 is solvent-dependent, the relaxation leads to a symmetry-broken locally excited CT state only in a polar medium, but to a symmetrically delocalized excited state in an apolar solvent. This fact accounts for the strong solvent influence on the transient absorption of **3**. Furthermore, as in apolar media there is only a reorganization of the S_1 state along the *y* coordinate, the fluorescence bandwidth is small in apolar solvents, but as in polar media there is a reorganization along both coordinates; the fluorescence signals are broad in polar solvents. The different behavior of **3** and **4** in apolar media is due to the influence of the methoxy and chloro substituents. The latter destabilize a polar symmetry-broken CT state. The strong coupling in **3** leads to significant differences of the spectral properties of dimer **3** and monomer **6**. For example, the oscillator strengths for fluorescence, f_{fl}, of **3** and **6** are about the same and, thus, are not additive. Furthermore, the estimated dipole moment differences, $\Delta\mu$, derived from the Lippert−Mataga plots of dimer **3** differ significantly from $\Delta\mu$ of **6**. The fluorescence quantum yields of anthracene monomer **6** is close to unity in most solvents and, therefore, k_{nr} is small. The quantum yields of corresponding anthracene dimer **3** are even smaller than that of monomer unit **6** in all solvents. This observation reflects that superradiant emission is found only if in the monomer k_{nr} is large and the quantum yield is small. Thus, superradiance is not visible in strongly coupled dimers such as **3** and **4** because the strong coupling results in nonadditive behavior of f_{fl}.

The excited-state mixed-valence compounds, **1**−**4**, as well as their corresponding monomers, **5** and **6**, investigated in this study exhibit different spectroscopic behavior in apolar and polar solvents. The Lippert−Mataga plots cannot be fitted by a single

linear function over the complete polarity range. However, not only dimers **1**−**4** show two different linear correlations, one for apolar or weakly polar and one for polar solvents, but also the corresponding monomers **5** and **6**. Consequently, this behavior cannot be traced back to interactions of the subunits in the dimers. Comparable results with bilinear Lippert−Mataga plots have been described already in the literature.[55,85−87] The bilinear Lippert−Mataga plots as well as the transient absorption properties of compounds **1**−**6** indicate a major molecular reorganization in the first excited states. In eq 9 the polarizability, α, of the molecule is neglected and the dipole is approximated as a point dipole in a spherical cavity of the solvent that is described by a dielectric continuum model.[66,67] These approximations and the fact that the molecules investigated here are not spherical may be the reason that the solvent influence on the first excited state is not described well and the plots are, thus, bilinear. A similar behavior was found for other organic molecules and in this context modified polarity scales were tested to improve the Lippert−Mataga equation.[85−87] In fact, what we found is that the use of another polarity scale still results in bilinear plots.

Conclusions

In this study we investigated a set of bistriarylamine D−π−D compounds **1**−**4**. Although superficially symmetrical, bistriarylamines **1** and **2** undergo a symmetry breaking in the excited state as can be seen from the ΔG^* values in Table 6. Although the accuracy of the computations is limited, the fact that a barrier was found supports this assumption. This symmetry breaking is stronger in polar solvents than in apolar solvents and is due to a weak electronic coupling of the monomeric subchromophores and a strong coupling to solvent modes, which increases the reorganization energy. Reactions on the excited-state adiabatic PES can be conceived as being excited-state hole-transfer processes from one triarylamine unit to the other, that is, as excited-state mixed-valence compounds. A further consequence of the weak electronic coupling is the superradiant behavior, particularly of **2**, which leads to an up to threefold enhancement of fluorescence quantum yield compared to monomer **5**. In contrast, anthracene derivatives **3** and **4** show a different behavior. Both **3** and **4**, exhibit a stronger electronic coupling than **1** and **2**, and the PES is solvent-dependent in a more subtle way: anthracene **3** with methoxy substituents attached to the triarylamine moieties shows a double minimum PES of the S_1 state in polar solvents while the barrier vanishes in apolar solvents and the excited state is delocalized. This shows that solvent influence is the symmetry breaking factor in these cases. Compound **4** with chloro substituents instead of methoxy exhibits a delocalized barrierless PES in all solvents. This observation demonstrates very nicely that even small modifications in the chromophore periphery may influence the photophysical behavior strongly. Anthracene dimers **3** and **4** both exhibit large fluorescence quantum yields in a large solvent polarity range and, furthermore, a large two-photon absorption cross section.[10] Thus, both molecules have suitable properties for two-photon applications.[88] Methoxy-substituted anthracene **3** might be an attractive material for two-photon pumped upconverted fiber lasing because the fluorescence and, thus, the lasing can be tuned by polarity of the dye solution.[88] Chloro-substituted anthracene **4**, however, is an interesting chromophore for two-photon confocal laser scanning microscopy because of its weak solvatochromism of the fluorescence.[88]

The excited-state PES of the anthracene compounds show a solvent dependence very similar to the ground state PES of $\mathbf{3}^+$ and $\mathbf{4}^+$ mixed-valence radical cations. This observation demonstrates the close analogy of excited-state mixed-valence behavior of neutral chromophores and the ground-state mixed-valence behavior of the radical cations derived thereof.

Acknowledgment. We are grateful to the Deutsche Forschungsgemeinschaft, the Volkswagenstiftung and the Graduiertenkolleg 1221 "Control of Electronic properties of Aggregated π-Conjugated Molecules" for financial support. We would also like to thank J. Pfister and M. Gsaenger for their assistance in some of the picosecond measurements.

References and Notes

(1) Hreha, R. D.; George, C. P.; Haldi, A.; Domercq, B.; Malagoli, M.; Barlow, S.; Brédas, J.-L.; Kippelen, B.; Marder, S. R. *Adv. Funct. Mater.* **2003**, *13*, 967−973.

(2) Albota, M.; Beljonne, D.; Brédas, J.-L.; Ehrlich, J. E.; Fu, J.-Y.; Heikal, A. A.; Hess, S. E.; Kogej, T.; Levin, M. D.; Marder, S. R.; McCord-Maughon, D.; Perry, J. W.; Rockel, H.; Rumi, M.; Subramaniam, G.; Webb, W. W.; Wu, X.-L.; Xu, C. *Science* **1998**, *281*, 1653−1656.

(3) Reinhardt, B. A.; Brott, L. L.; Clarson, S. J.; Dillard, A. G.; Bhatt, J. C.; Kannan, R.; Yuan, L. X.; He, G. S.; Prasad, P. N. *Chem. Mater.* **1998**, *10*, 1863−1874.

(4) Rumi, M.; Ehrlich, J. E.; Heikal, A. A.; Perry, J. W.; Barlow, S.; Hu, Z.; McCord-Maughon, D.; Parker, T. C.; Roeckel, H.; Thayumanavan, S.; Marder, S. R.; Beljonne, D.; Brédas, J.-L. *J. Am. Chem. Soc.* **2000**, *122*, 9500−9510.

(5) Chung, S. J.; Lin, T. C.; Kim, K. S.; He, G. S.; Swiatkiewicz, J.; Prasad, P. N.; Baker, G. A.; Bright, F. V. *Chem. Mater.* **2001**, *13*, 4071−4076.

(6) Cho, B. R.; Piao, M. J.; Son, K. H.; Lee, S. H.; Yoon, S. J.; Jeon, S. J.; Cho, M. H. *Chem.−Eur. J.* **2002**, *8*, 3907−3916.

(7) Pond, S. J. K.; Rumi, M.; Levin, M. D.; Parker, T. C.; Beljonne, D.; Day, M. W.; Brédas, J. L.; Marder, S. R.; Perry, J. W. *J. Phys. Chem. A* **2002**, *106*, 11470−11480.

(8) Yang, W. J.; Kim, C. H.; Jeong, M. Y.; Lee, S. K.; Piao, M. J.; Jeon, S. J.; Cho, B. R. *Chem. Mater.* **2004**, *16*, 2783−2789.

(9) Ortiz, R. P.; Delgado, M. C. R.; Casado, J.; Hernandez, V.; Kim, O. K.; Woo, H. Y.; Navarrete, J. T. L. *J. Am. Chem. Soc.* **2004**, *126*, 13363−13376.

(10) Strehmel, B.; Amthor, S.; Schelter, J.; Lambert, C. *ChemPhysChem* **2005**, *6*, 893−896.

(11) Lambert, C.; Nöll, G.; Schelter, J. *Nat. Mater.* **2002**, *1*, 69−73.

(12) Amthor, S.; Lambert, C. *J. Phys. Chem. A* **2006**, *110*, 1177−1189.

(13) Lambert, C.; Amthor, S.; Schelter, J. *J. Phys. Chem. A* **2004**, *108*, 6474−6486.

(14) Amthor, S.; Noller, B.; Lambert, C. *Chem. Phys.* **2005**, *316*, 141−152.

(15) Fraysse, S.; Coudret, C.; Launay, J. P. *Tetrahedron Lett.* **1998**, *39*, 7873−7876.

(16) Schlicke, B.; De Cola, L.; Belser, P.; Balzani, V. *Coord. Chem. Rev.* **2000**, *208*, 267−275.

(17) Schenning, A. P. H. J.; Tsipis, A. C.; Meskers, S. C. J.; Beljonne, D.; Meijer, E. W.; Brédas, J. L. *Chem. Mater.* **2002**, *14*, 1362−1368.

(18) Fraysse, S.; Coudret, C.; Launay, J.-P. *J. Am. Chem. Soc.* **2003**, *125*, 5880−5888.

(19) Zareie, M. H.; Ma, H.; Reed, B. W.; Jen, A. K. Y.; Sarikaya, M. *Nano Lett.* **2003**, *3*, 139−142.

(20) Giacalone, F.; Segura, J. L.; Martin, N.; Guldi, D. M. *J. Am. Chem. Soc.* **2004**, *126*, 5340−5341.

(21) Kang, S. H.; Ma, H.; Kang, M. S.; Kim, K. S.; Jen, A. K. Y.; Zareie, M. H.; Sarikaya, M. *Angew. Chem., Int. Ed.* **2004**, *43*, 1512−1516.

(22) Walter, D.; Neuhauser, D.; Baer, R. *Chem. Phys.* **2004**, *299*, 139−145.

(23) Heilbronner, E.; Maier, J. P. *Helv. Chim. Acta* **1974**, *57*, 151−159.

(24) Canuto, S.; Zerner, M. C. *Chem. Phys. Lett.* **1989**, *157*, 353−358.

(25) Canuto, S.; Zerner, M. C. *J. Am. Chem. Soc.* **1990**, *112*, 2114−2120.

(26) Bazan, G. C.; Oldham, J., Jr.; Lachicotte, R. J.; Tretiak, S.; Chernyak, V.; Mukamel, S. *J. Am. Chem. Soc.* **1998**, *120*, 9188−9204.

(27) Verdal, N.; Godbout, J. T.; Perkins, T. L.; Bartholomew, G. P.; Bazan, G. C.; Kelley, A. M. *Chem. Phys. Lett.* **2000**, *320*, 95−103.

(28) Zyss, J.; Ledoux, I.; Volkov, S.; Chernyak, V.; Mukamel, S.; Bartholomew, G. P.; Bazan, G. C. *J. Am. Chem. Soc.* **2000**, *122*, 11956−11962.

(29) Bartholomew, G. P.; Bazan, G. C. *Acc. Chem. Res.* **2001**, *34*, 30−39.

(30) Bartholomew, G. P.; Bazan, G. C. *J. Am. Chem. Soc.* **2002**, *124*, 5183−5196.
(31) Moran, A. M.; Bartholomew, G. P.; Bazan, G. C.; Kelley, A. M. *J. Phys. Chem. A* **2002**, *106*, 4928−4937.
(32) Bartholomew, G. P.; Rumi, M.; Pond, S. J. K.; Perry, J. W.; Tretiak, S.; Bazan, G. C. *J. Am. Chem. Soc.* **2004**, *126*, 11529−11542.
(33) Leng, W.; Grunden, J.; Bartholomew, G. P.; Bazan, G. C.; Kelley, A. M. *J. Phys. Chem. A* **2004**, *108*, 10050−10059.
(34) Grimme, S. *Chem.—Eur. J.* **2004**, *10*, 3423−3429.
(35) Hong, J. W.; Woo, H. Y.; Liu, B.; Bazan, G. C. *J. Am. Chem. Soc.* **2005**, *127*, 7435−7443.
(36) Woo, H. Y.; Hong, J. W.; Liu, B.; Mikhailovsky, A.; Korystov, D.; Bazan, G. C. *J. Am. Chem. Soc.* **2005**, *127*, 820−821.
(37) Guyard, L.; Nguyen Dinh An, M.; Audebert, P. *Adv. Mater.* **2001**, *13*, 133−136.
(38) Guyard, L.; Audebert, P. *Electrochem. Commun.* **2001**, *3*, 164−167.
(39) Morisaki, Y.; Chujo, Y. *Macromolecules* **2002**, *35*, 587−589.
(40) Morisaki, Y.; Ishida, T.; Chujo, Y. *Macromolecules* **2002**, *35*, 7872−7877.
(41) Morisaki, Y.; Chujo, Y. *Chem. Lett.* **2002**, 194−195.
(42) Salhi, F.; Lee, B.; Metz, C.; Bottomley, L. A.; Collard, D. M. *Org. Lett.* **2002**, *4*, 3195−3198.
(43) Salhi, F.; Collard, D. M. *Adv. Mater.* **2003**, *15*, 81−85.
(44) Morisaki, Y.; Chujo, Y. *Macromolecules* **2003**, *36*, 9319−9324.
(45) Morisaki, Y.; Fujimura, F.; Chujo, Y. *Organometallics* **2003**, *22*, 3553−3557.
(46) Morisaki, Y.; Chujo, Y. *Macromolecules* **2004**, *37*, 4099−4103.
(47) Morisaki, Y.; Ishida, T.; Tanaka, H.; Chujo, Y. *J. Polym. Sci., Part A: Polym. Chem.* **2004**, *42*, 5891−5899.
(48) Morisaki, Y.; Chujo, Y. *Bull. Chem. Soc. Jpn.* **2005**, *78*, 288−293.
(49) Morisaki, Y.; Wada, N.; Chujo, Y. *Polymer* **2005**, *46*, 5884−5889.
(50) Miller, D. S.; Leffler, J. E. *J. Phys. Chem.* **1970**, *74*, 2571−2574.
(51) Leroy, E.; Lami, H. *Chem. Phys. Lett.* **1976**, *41*, 373−377.
(52) Yao, H.; Okada, T.; Mataga, N. *J. Phys. Chem.* **1989**, *93*, 7388−7394.
(53) Lueck, H. B.; McHale, J. L.; Edwards, W. D. *J. Am. Chem. Soc.* **1992**, *114*, 2342−2348.
(54) Lewis, L. M.; Indig, G. L. *Dyes Pigm.* **2000**, *46*, 145−154.
(55) Piet, J. J.; Schuddeboom, W.; Wegewijs, B. R.; Grozema, F. C.; Warman, J. M. *J. Am. Chem. Soc.* **2001**, *123*, 5337−5347.
(56) Zhang, F. S.; Lynden-Bell, R. M. *Phys. Rev. Lett.* **2003**, *90*, 185505.
(57) Cisnetti, F.; Ballardini, R.; Credi, A.; Gandolfi, M. T.; Masiero, S.; Negri, F.; Pieraccini, S.; Spada, G. P. *Chem.—Eur. J.* **2004**, *10*, 2011−2021.
(58) Ortiz, R. P.; Delgado, M. C. R.; Casado, J.; Hernández, V.; Kim, O. K.; Woo, H. Y.; Navarrete, J. T. L. *J. Am. Chem. Soc.* **2004**, *126*, 13363−13376.
(59) Thompson, A. L.; Gaab, K. M.; Xu, J. J.; Bardeen, C. J.; Martínez, T. J. *J. Phys. Chem. A* **2004**, *108*, 671−682.
(60) Karstens, T.; Kobs, K. *J. Phys. Chem. A* **1980**, *84*, 1871−1872.
(61) Gurzadyan, G. G.; Steenken, S. *Chem.—Eur. J.* **2001**, *7*, 1808−1815.
(62) Gurzadyan, G.; Gorner, H. *Chem. Phys. Lett.* **2000**, *319*, 164−172.
(63) Birks, J. *Photophysics of Aromatic Molecules*; Wiley-Interscience: London, 1970.
(64) Lewis, J. E.; Maroncelli, M. *Chem. Phys. Lett.* **1998**, *282*, 197−203.
(65) Strickler, S. J.; Berg, R. A. *J. Chem. Phys.* **1962**, *37*, 814.
(66) Mataga, N.; Kaifu, Y.; Koizumi, M. *Bull. Chem. Soc. Jpn.* **1956**, *29*, 465−470.
(67) Lippert, E. *Z. Elektrochem.* **1957**, *61*, 962−975.
(68) Lampert, R. A.; Chewter, L. A.; Phillips, D.; O'Connor, D. V.; Roberts, A. J.; Meech, S. R. *Anal. Chem.* **1983**, *55*, 68−73.
(69) Levitus, M.; Garcia-Garibay, M. A. *J. Phys. Chem. A* **2000**, *104*, 8632−8637.
(70) Lambert, C.; Schelter, J.; Fiebig, T.; Mank, D.; Trifonov, A. *J. Am. Chem. Soc.* **2005**, *127*, 10600−10610.
(71) Dümmler, S.; Roth, W.; Fischer, I.; Heckmann, A.; Lambert, C. *Chem. Phys. Lett.* **2005**, *408*, 264−268.
(72) Badger, B.; Brocklehurst, B. *Trans. Faraday Soc.* **1969**, *65*, 2582−2587.
(73) Shida, T. *Electronic Absorption Spectra of Radical Ions*; Elsevier: Amsterdam, 1988; Vol. 34.
(74) Ruseckas, A.; Namdas, E. B.; Lee, J. Y.; Mukamel, S.; Wang, S. J.; Bazan, G. C.; Sundström, V. *J. Phys. Chem. A* **2003**, *107*, 8029−8034.
(75) Anthracene bridged donor-bridge and donor-bridge-acceptor compounds with a charge-separated excited state have been discussed in the literature, but the transient absorption spectra were only recorded above 12 500 cm^{-1}.[76−79]
(76) Kilsa, K.; Macpherson, A. N.; Gillbro, T.; Martensson, J.; Albinsson, B. *Spectrochim. Acta, Part A* **2001**, *57*, 2213−2227.
(77) Kilsa, K.; Kajanus, J.; Macpherson, A. N.; Martensson, J.; Albinsson, B. *J. Am. Chem. Soc.* **2001**, *123*, 3069−3080.
(78) Pettersson, K.; Kilsa, K.; Martensson, J.; Albinsson, B. *J. Am. Chem. Soc.* **2004**, *126*, 6710−6719.
(79) Winters, M. U.; Pettersson, K.; Martensson, J.; Albinsson, B. *Chem.—Eur. J.* **2005**, *11*, 562−573.
(80) In principle, low-lying locally excited anthracene states (see section Picosecond Time-Resolved Transient Absorption Spectroscopy) have to be considered for a better description of the PESs of anthracene compounds **3** and **4** because an interaction of anthracene states and the two degenerate excited CT states may be possible. Unfortunately, we lack of any experimental data that would allow us to quantify the interaction (coupling) between the excited anthracene states and the excited CT states. Thus, our simple model is restricted to the ground state and the two excited CT states for all compounds. We suppose that this three-state model is suitable for the description of the PESs because the spectroscopic properties of all bistriarylamines are reproduced well by this model.
(81) Fischer, G. *Vibronic Coupling*; Academic Press: London, 1984.
(82) Dattelbaum, D. M.; Hartshorn, C. M.; Meyer, T. J. *J. Am. Chem. Soc.* **2002**, *124*, 4938−4939.
(83) Rehler, N. E.; Eberly, J. H. *Phys. Rev. A* **1971**, *3*, 1735−1751.
(84) Gnanakaran, S.; Haran, G.; Kumble, R.; M, H. R. In *Resonance Energy Transfer*; Demidov, A. A., Andrews, D. L., Eds.; Wiley: Chichester, 1999; pp 308−365.
(85) Verbeek, G.; Depaemelaere, S.; Van der Auweraer, M.; De Schryver, F. C.; Vaes, A.; Terrell, D.; De Meutter, S. *Chem. Phys.* **1993**, *176*, 195−213.
(86) Catalán, J.; Díaz, C.; López, V.; Perez, P.; Claramunt, R. M. *J. Phys. Chem.* **1996**, *100*, 18392−18398.
(87) Onkelinx, A.; DeSchryver, F. C.; Viaene, L.; VanderAuweraer, M.; Iwai, K.; Yamamoto, M.; Ichikawa, M.; Masuhara, H.; Maus, M.; Rettig, W. *J. Am. Chem. Soc.* **1996**, *118*, 2892−2902.
(88) Bhawalkar, J. D.; He, G. S.; Prasad, P. N. *Rep. Prog. Phys.* **1996**, *59*, 1041−1070.